Case Studies in Thermal Engineering 32 (2022) 101899

Contents lists available at ScienceDirect

Case Studies in Thermal Engineering

journal homepage: www.elsevier.com/locate/csite

Exergy analysis in a HCCI engine operated with diethyl ether-fusel oil blends

Juan Zapata-Mina [a,*], Seyed Mohammad Safieddin Ardebili [b], Alvaro Restrepo [a], Hamit Solmaz [c], Alper Calam [d], Özer Can [e]

[a] Faculty of Mechanical Engineering, Technological University of Pereira, Colombia
[b] Department of Biosystems Engineering, Shahid Chamran University of Ahvaz, Ahvaz, Iran
[c] Automotive Engineering Department, Faculty of Technology, Gazi University, Ankara, Turkey
[d] Technical Sciences Vocational High School, Gazi University, Ankara, Turkey
[e] Automotive Engineering Department, Faculty of Technology, Pamukkale University, Denizli, Turkey

ARTICLE INFO

Keywords:
Exergy analysis
HCCI engine
Diethyl ether
Fusel oil

ABSTRACT

Homogeneous Charge compression ignition (HCCI) combustion mode is a very interesting new combustion model with high efficiency, low nitrogen oxide (NOx), and soot emissions. In the present investigation, the performance of an HCCI engine operated with three fuel ratios, i.e., 40% diethyl ether and 60% fusel oil (D40F60), 60% diethyl ether and 40% fusel oil (D60F40), and 80% diethyl ether and 20% fusel oil (D80F20), at different lambda values and engine speeds was assessed from exergy indicators. The results indicate that the lambda variation allows observing the best performance zones when operating with fuel blends. From the comparison of the exergy indicators, it is concluded that the highest engine efficiency is obtained when operating with D40F60 at a lambda between 2.1 and 2.2. However, it was determined that the increase of diethyl ether in the blend decreases the HCCI engine performance. Also, greater stability of performance was recorded when operating with D80F20. A higher exergy destruction rate is observed between lambda 3.4 and 3.9 when operating with D80F20. The exergetic efficiency values varied from 5.34% to 23.85%. According to the results obtained, the lowest and highest value of exergy efficiency was recorded for the D80F20 and D40F60, respectively.

Nomenclature

D40F60	40% diethyl ether and 60% fusel oil
D60F40	60% diethyl ether and 40% fusel oil
D80F20	80% diethyl ether and 20% fusel oil
λ	relative air-fuel ratio [−]
$\dot{E}x_{in}$	input exergy rates [kW]
$\dot{E}x_{out}$	output exergy rates [kW]
$\dot{E}x_{D}$	exergy destroyed rate[kW]

* Corresponding author.
E-mail addresses: juan.zapata1@utp.edu.co (J. Zapata-Mina), m.safieddin@scu.ac.ir (S.M. Safieddin Ardebili), arestrep@utp.edu.co (A. Restrepo), hsolmaz@gazi.edu.tr (H. Solmaz), acalam@gazi.edu.tr (A. Calam), ozercan@pau.edu.tr (Ö. Can).

https://doi.org/10.1016/j.csite.2022.101899
Received 17 January 2022; Received in revised form 18 February 2022; Accepted 21 February 2022
Available online 26 February 2022

$\dot{E}_{in}$	input energy rates [kW]
$\dot{E}_{out}$	output energy rates [kW]
$\dot{m}_{air}$	mass of the air, [kg/s]
$c_{p,air}$	heat capacity of the input air, [kJ/kg-K]
T_{air}	air temperature, [K]
T_{amb}	ambient temperature, [K]
$\dot{m}_{fuel}$	mass of the fuel, [kg/s]
LHV	lower heating value of the fuel, [kJ/kg]
φ	chemical exergy factor [−]
N	engine speed, [rpm]
T	engine torque, [Nm]
$ex_{exh,ph}$	physical exergy rate [kW]
$ex_{exh,che}$	chemical exergy rate [kW]
$c_{p,i}$	heat capacity, [kJ/kg-K]
R_u	universal gas constant
y_i	molar fraction [−]
x_i	mass fraction [−]
M_i	molar mass [kg/kmol]
T_{vc}	control volume temperature, [K]
$\dot{Q}_{loss}$	heat loss rate [kW]

1. Introduction

The world is rapidly polluted with the increasing population and developing industrialization. The main liable of this is petroleum-based energy resources. Since petroleum based fuels are used in internal combustion engines, they cause high exhaust emission and rapidly pollute the atmosphere. Therefore, researchers continue to work on alternative fuels with cleaner combustion products and new combustion models to be used in the automotive industry [1–6].

Homogeneous Charge Compression Ignition (HCCI) combustion mode is an interesting, and new combustion model with high efficiency, low nitrogen oxide (NOx), and soot emissions. In the HCCI engines, the lean and homogeneous air/fuel mixture is compressed in a high compression ratio engine. As a result, a spontaneous combustion occurs in the combustion chamber [7–9]. Theoretically, in HCCI engines, compared to conventional diesel combustion, regional rich mixture and high temperature flame zones do not occur. Thus, while maintaining high thermal efficiency, NOx and soot emissions are low at the same time [10–13]. Since combustion occurs spontaneously in HCCI engines, the chemical kinetics of the air/fuel mixture plays an active role in the combustion processes. Control of chemical kinetics are affected on parameters such as engine operating range, combustion start, burning time, thermal efficiency [14,15]. Therefore, the physical and chemical properties of the fuel or fuel blends to be used in HCCI engines can enable the ignition timing to be controlled [16,17]. However, the ringing problem should be overcome by slowing down the fast oxidation reactions. In addition, the problem of misfire occurs at low engine loads [18,19]. HCCI combustion duration and start of combustion can be controlled by variables such as low reactivity fuel usage [20,21], exhaust gas recirculation (EGR) [22,23], negative valve overlap [24,25]. Solving the misfire problem at low loads depends on parameters such as high reactivity fuel use [26,27], variable compression ratio [28,29], control of intake air inlet temperature [30,31]. The researchers stated that it would be beneficial to change two of the above-mentioned parameters together in order to solve these problems simultaneously [32–34]. Maurya and Agarwal [35] studied the effects of low reactivity alternative fuels (ethanol and methanol) on HCCI combustion at different intake air inlet temperatures. They revealed that alcohols with the high latent heat of vaporization must be heated to at least 160 ^{o}C in order for the oxidation reactions to occur spontaneously in the cylinder. Solmaz [21] examined the effects on HCCl combustion at different compression ratios by mixing low reactivity fusel oil with high reactivity n-heptane. It was revealed that the compression ratio has a significant effect on the combustion of HCCI, and also it can be used to control the combustion phase of low and high reactivity blended fuels. Calam [20] studied the effects of low and high reactivity (fusel oil + n-heptane) fuels with different mixing ratios on HCCI combustion at different intake air inlet temperatures. He stated that the combustion phase could be controlled by low reactivity fuels at high intake air inlet temperature. Wang et al. [36] examined the effects of polyoxymethylene dimethyl ether fuels with different cetane numbers on HCCI combustion at different engine loads and EGR rates. While the increase in the engine load allowed the start of the combustion to be advanced, the increase in the EGR rate delayed the start of the combustion. The composition of the homogeneous mixture and the EGR rate are two important parameters for controlling the start of combustion. Uyumaz [37] studied the effects of mixtures of isopropanol and n-butanol with various volumes of n-heptane fuel on HCCl combustion. This study was conducted at five different intake air inlet temperatures. The increase in isopropanol and n-butanol in blending fuels enabled the low-temperature oxidation phase (LTO) to be controlled. This extended the combustion duration, and no HCCI knock occurred. Also, the change in the intake air temperature significantly controlled the start of combustion.

Exergy analysis of thermal systems such as internal combustion engines has become an increasingly interesting topic as possible causes of waste energy reduction can be identified [38]. It was stated above that combustion can be controlled in HCCI engines using

Table 1
Engine specifications.

Test Engine	
Number of cylinders	1
Intake valve O/C timing	12° bTDC 56° aBDC
Exhaust valve O/C timing	56° bBDC 12° aTDC
Swept volume [cm^3]	540
Compression ratio	13
Bore [mm] × Stroke [mm]	80.26 x 88.90
Maximum power output (kW)	15
Valve lift Intake-Exhaust [mm]	5.5–3.5
Combustion mode	HCCI

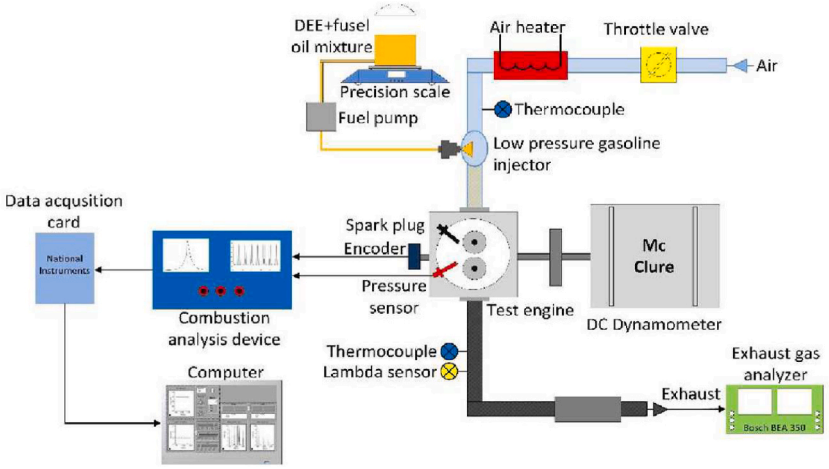

Fig. 1. Schematic view of the testbed.

dual fuel. Therefore, in the use of dual fuels in HCCI engines, heat losses should be analyzed as well as controlling the combustion processes [39]. Taghavifar et al. [40], strived to examine the effect of different DME fuel mixtures (i.e., D80M20, D70M20DME10, D60M10DME30, and D50M30DME20) in an HCCI engine. In terms of exergy performance, they claimed that the D50M30DME20 fuel was the optimal fuel ratio. In a different study, Zhang et al. [41], compared the exergy losses of the auto-ignition process for MeOH and EtOH blended with DME based on the second-law thermodynamic. They concluded that the addition of DME/methanol could increase the exergy losses by the H_2O_2 loop reactions. Khaliq et al. [19] employed the combined first law and the second law of thermodynamic method for an HCCI engine fueled with wet ethanol. Their findings revealed maximum exergy of ~ 90.09% of the total exergy destruction was destroyed in the HCCI engine. They also highlighted a reduction in the exergy losses and the irreversibility when the initial charge temperature increased. In an interesting study, the impact of EGR on the work exergy of an HCCI engine operated with the blend of biodiesel and diesel was taken into account by Jafarmadar et al. [42]. They reported that the accumulative work exergy decreased by 2.9% with increasing EGR mass fraction up to 30%. They argued that blending biodiesel into net diesel led to a decrease in accumulative heat loss exergy, while irreversibility increased. In a different study comparing the exergetic efficiencies and fuel consumption of an HCCI engine, an exergetic efficiency of up to 80% were recorded, which this high efficiency resulted in a reduction of 40% in the fuel consumption compared to the separately produced hydrogen/heat/power [43]. Addition of a mixture of CO and hydrogen as a reformer gas on the exergy analysis of an HCCI engine operated with n-heptan and iso-octane as a fuel additive has been investigated by Neshat et al. [44]. They used different percentages of reformer gas ranging from 0% to 30%. They stated that the chemical effects had a higher effect in comparison with dilution and thermodynamic effects. They showed that the optimal value of the first law and second law efficiencies were obtained when 5%–10% of the reformer gas was utilized. Also, Eyal and Tartakovsky [45] conducted a study on the effects of reformer intercooling and bypassing a portion of the exhaust stream leaving the reformer in a compression ignition engine which they call RefCCI. In the work, they perform a second law analysis, focused on the calculation of the exergy destruction of the different components involved in the system and propose strategies to optimize the process.

For the above mentioned, this study presents the results of an exergy analysis on an HCCI engine operating with fusel oil and diethyl ether blends. Tests were performed on a single-cylinder HCCI engine operated with three fuel ratios (D40F60, D60F40 and D80F20) at different lambda values and engine speeds. The results were evaluated from exegetic indicators, from which engine exergy maps were built. The results obtained indicated that the lambda variation allows observing the best performance zones when operating with fuel blends. Likewise, greater engine performance stability was observed when operating with D80F20. However, when the engine was operated with lambda between 3.4 and 3.9, the highest exergy destruction rate was observed for the D80F20 fuel. Also, according to the results, the lowest and highest exergy efficiency values were recorded for D80F20 and D40F60, respectively.

Table 2
Volumetric content of blend fuels.

	Diethyl ether (%)	Fusel oil (%)
D40F60	40	60
D60F40	60	40
D80F20	80	20

Table 3
Specifications of test fuels [46,47].

Fuel	Fusel Oil	Diethyl ether
Water content [%]	10.3	1.46
Cetane number	–	>125
LHV [MJ/kg]	29.5	33.8
Density [kg/m^3]	849	713.4
Heat of vaporization [kJ/kg]	501	376
Research octane number	106.8	–
Chemical formula	$C_5H_{12}O$	$C_4H_{10}O$
Self-ignition temperature [°C]	416	160

2. Methodology

2.1. Experimental setup

In this study, an HCCI–SI test engine with a single-cylinder, four-stroke, port injection system was used. The test engine was connected to a DC dynamometer capable of absorbing 30 kW of power. The features of the test engine are shown in Table 1, and the schematic view of the test setup is shown in Fig. 1.

Fusel oil and diethyl ether were blended volumetrically in various proportions and used in HCCI engine. The mixture of test fuels was prepared with an ultrasonic mixer. At the end of 48 h, no phase separation was observed in the test fuels, and the experiments were carried out. Blend fuels were injected from the port injection system using a single injector. The content of the fuels and the abbreviations used are shown in Table 2.

Fusel oil as a by-product in the ethyl alcohol production process is very attractive to use in spark-ignition and HCCI engines mainly due to its high octane number. Main chemical/physical charactristics of the studied fuels are tabulated in Table 3.

The experiments were conducted using fusel oil/diethyl ether blends at a constant intake air inlet temperature of 353 K, varying the engine speed and air-fuel ratio as shown in Table 4. Some modifications were made to the test engine and it was converted to HCCI mode. During the tests, the HCCI mode throttle was placed in the full open position and the engine load was controlled by the air-fuel ratio.

It should be noted that when the engine was running on D40F60, the lambda value could not be stabilized for some engine speeds. Since, when the engine operates with lower dietileter content, the mixture fails to stabilize easily in combustion, due to the high volatility of the fuel which creates vapor bubbles and causes vapor lock in the fuel lines, this phenomenon occurs mainly when operating at high engine speeds and loads [48]. Therefore, lower operating points are observed with the D40F60 fuel.

2.2. Exergy model

To calculate the associated exergy rates and derive the charactristics of the combustion products, it is essential to determine the composition of the combustion products from Eq. (1) [49].

$$\alpha C_xH_yO_z + \beta C_pH_qO_r + \lambda a(O_2 + 3,773N_2) \rightarrow bCO_2 + cCO + eNO + fH_2O + gN_2 + hO_2 \quad (1)$$

where, α and β ($\alpha + \beta = 1$) stand for the fuel ratio in the blends. Also, z, y, x, r, q, and p refer to the fraction of each chemical term in the base fuels. λa are the relative air-fuel ratio and stoichiometric air coefficient, respectively. The remain parameters are considered as coefficients of combustion products. The value of b, c and e were derived from gas analyser. The following formulas was utilized to determine the coefficients.

$$\text{Hydrogen:}\quad \alpha y + \beta q = 2f \quad (2)$$

$$\text{Nitrogen:}\quad 6,773\lambda\left[\alpha\left(x + \frac{y}{4} - \frac{z}{2}\right) + \beta\left(p + \frac{q}{4} - \frac{r}{2}\right)\right] = e + 2g \quad (3)$$

$$\text{Oxygen:}\quad \alpha z + \beta r + 2\lambda\left[\alpha\left(x + \frac{y}{4} - \frac{z}{2}\right) + \beta\left(p + \frac{q}{4} - \frac{r}{2}\right)\right] = 2b + c + e + f + 2h \quad (4)$$

In order to evaluate the energy input/output in the combustion process, an external exergy analysis was performed [50,51]. The external exergy analysis model considers multiple physical variables such as temperature, rotational speed, fuel consumption, among others, to facilitate the calculation of performance indicators. For the analysis was considered a control volume in steady state. Moreover, for developing the exergy model, the exhaust gases and combustion air were considered as a ideal gas mixtures and change

Table 4
Operating conditions evaluated on the engine.

D40F60		D60F40		D80F20	
N	Lambda	N	Lambda	N	Lambda
[rpm]	[−]	[rpm]	[−]	[rpm]	[−]
800	2.3	800	3.15	800	3.15
800	2.1	800	2.9	800	2.9
800	2	800	2.65	800	2.7
800	1.8	800	2.45	800	2.5
800	1.65	800	2.25	800	2.3
800	1.55	800	2.1	800	2.15
800	1.4	800	2	800	2
800	2.2	800	1.8	800	1.9
1000	1.8	800	1.4	800	1.8
1000	1.55	1000	3.4	1000	3
1000	1.4	1000	3.1	1000	2.8
1100	1.8	1000	2.85	1000	2.6
1100	1.8	1000	2.6	1000	2.4
1100	1.8	1000	2.4	1000	2.2
1100	1.8	1000	2.25	1000	2.05
1100	1.8	1000	2.1	1000	1.95
1100	1.4	1000	1.8	1000	1.8
1100	1.35	1000	1.4	1100	3.05
1200	1.5	1100	1.4	1100	2.8
1200	1.4	1100	2.2	1200	2.6
1400	2.2	1100	3	1200	2.4
1400	1.4	1100	2.75	1200	2.2
1400	2.2	1100	2.5	1200	2.05
1400	1.8	1100	2.3	1200	1.9
–	–	1100	2.15	1200	1.8
–	–	1200	2	1200	3.4
–	–	1200	1.8	1200	3.1
–	–	1200	2.95	1400	2.8
–	–	1200	2.7	1400	2.6
–	–	1200	2.5	1400	2.45
–	–	1200	2.3	1400	2.3
–	–	1200	2.1	1400	2.1
–	–	1400	1.8	1400	2
–	–	1400	3.2	1400	1.9
–	–	1400	3	1400	1.8
–	–	1400	2.8	1400	4
–	–	1400	2.55	1400	3.7
–	–	1400	1.8	1600	3.5
–	–	1400	1.8	1600	3.3
–	–	1400	1.8	1600	3.1
–	–	1600	1.8	1600	3.35
–	–	1600	1.8	1600	3.1
–	–	1600	2.2	1800	2.2
–	–	1800	1.4	1800	1.4

in kinetic/potential exergy disregared [52–54]. The thermodynamic reference state for pressure and temperature are selected: $P_0 = 101,325$ kPa and $T_0 = 298,15$ K. Eqs. (5)–(7) present the mass, exergy and energy balance respectively. The schematic of the exergy balance of an internal comustion engine is depicted in Fig. 2.

$$\sum \dot{m}_{in} = \sum \dot{m}_{out} \tag{5}$$

$$\sum \dot{E}x_{in} = \sum \dot{E}x_{out} + \dot{E}x_D \tag{6}$$

$$\sum \dot{E}_{in} = \sum \dot{E}_{out} \tag{7}$$

In addition, in terms of the air inputs into the system and the fuel, the exergy rate could be expressed by Eqs. (8)–(10).

$$\dot{E}x_{air} = \dot{m}_{air}\left[c_{p,air}\left((T_{air} - T_0) - T_0 ln ln\left(\frac{T_{air}}{T_0}\right)\right)\right] \tag{8}$$

$$\dot{E}x_{fuel} = \dot{m}_{fuel} LHV \varphi \tag{9}$$

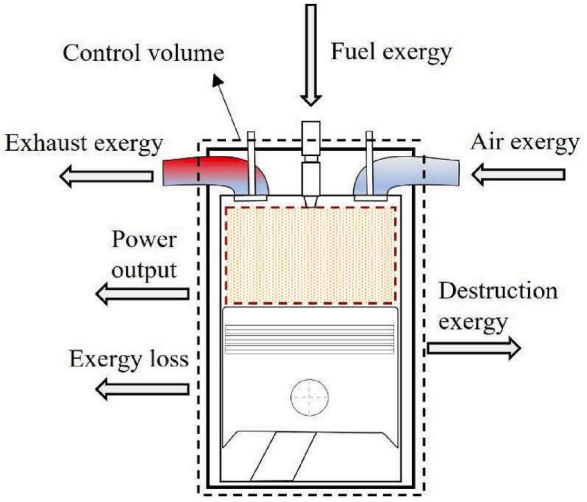

Fig. 2. Exergy balance scheme.

Table 5
Mass fractions of fuels evaluated.

	D40F60	D60F40	D80F20
Carbon content [−]	0.6686	0.6619	0.6553
Hydrogen content [−]	0.1359	0.1356	0.1354
Oxygen content [−]	0.1956	0.2025	0.2093
Sulfur content [−]	0.0001	0.0001	0.0001
φ [−]	1.088	1.089	1.090

Table 6
Definition of the environment [55].

Reference component	Molar fraction [%]
CO_2	0.03450
O_2	20.35000
N_2	75.67000
CO	0.00070
H_2O	3.03000
NO	0.00001
Others	0.91479

$$\varphi = 1.0401 + 0.1728\left(\frac{H}{C}\right) + 0.0432\left(\frac{O}{C}\right) + 0.2169\left(\frac{S}{C}\right)\left(1 - 2.2068\frac{H}{C}\right) \tag{10}$$

where, O, S , H, and, C stand for mass fractions of the oxygen, sulfur contents, hydrogen, and carbon of the fuel, respectively, and the accuracy of this equation is estimated as ±0.38% (see Table 5) [50,51].

The exergy rate of useful power output could be determined with Eq. (11).

$$\dot{E}x_W = \dot{W} = \frac{2\pi N}{60}T \tag{11}$$

In terms of the exhaust gases, in order to calculate the exergy rate, the sumision of physical/chemical exergy was used as illustrated in Eqs. (12)–(14).

$$\dot{E}x_{exh} = \left(\dot{m}_{fuel} + \dot{m}_{air}\right)\left(ex_{exh,ph} + ex_{exh,che}\right) \tag{12}$$

$$ex_{exh,ph} = c_{p,i}\left[\left(T_{exh} - T_0\right) - T_0 ln\left(\frac{T_{exh}}{T_0}\right)\right] \tag{13}$$

$$ex_{exh,che} = R_u T_0 \sum_i \frac{x_i}{M_i} ln\ \frac{y_i}{y_{i,0}} \tag{14}$$

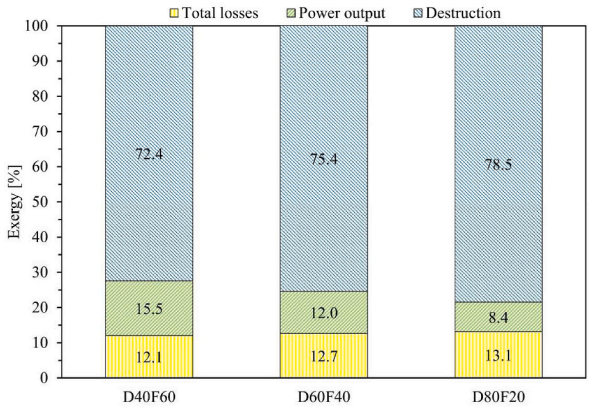

Fig. 3. Exergy balance average of all conditions.

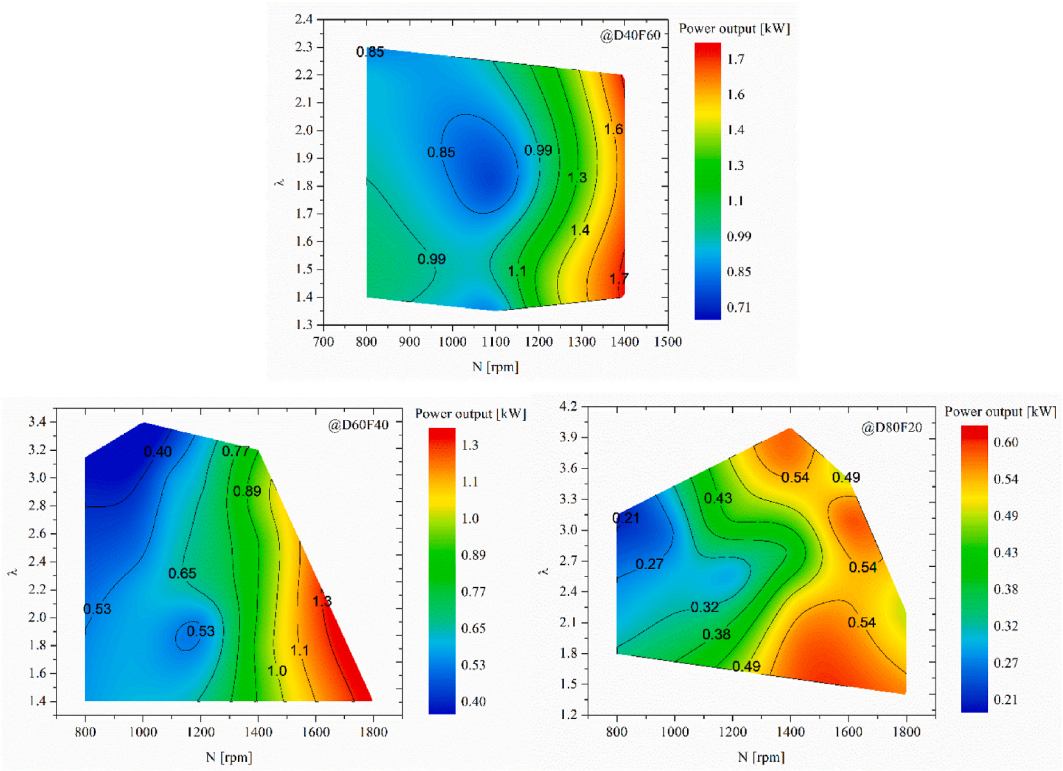

Fig. 4. Power output in relation to lambda and rotational speed.

The definition of the environment is shown in Table 6.

The following Eqs. (15)–(17) were employed to compute the exergy loss rate, destruction exergy, second law efficiency, and waste exergy of the engine respectively.

$$\dot{E}x_{loss} = \dot{Q}_{loss}\left(1 - \frac{T_0}{T_{vc}}\right) \tag{15}$$

where, T_{vc} corresponds to the control volume temperature which is an average of the block temperature and oil temperature.

$$\dot{E}x_D = \dot{E}x_{air} + \dot{E}x_{fuel} - \dot{E}x_W - \dot{E}x_{exh} - \dot{E}x_{loss} \tag{16}$$

$$\psi = \frac{\dot{E}x_W}{\dot{E}x_{fuel} + \dot{E}x_{air}} \tag{17}$$

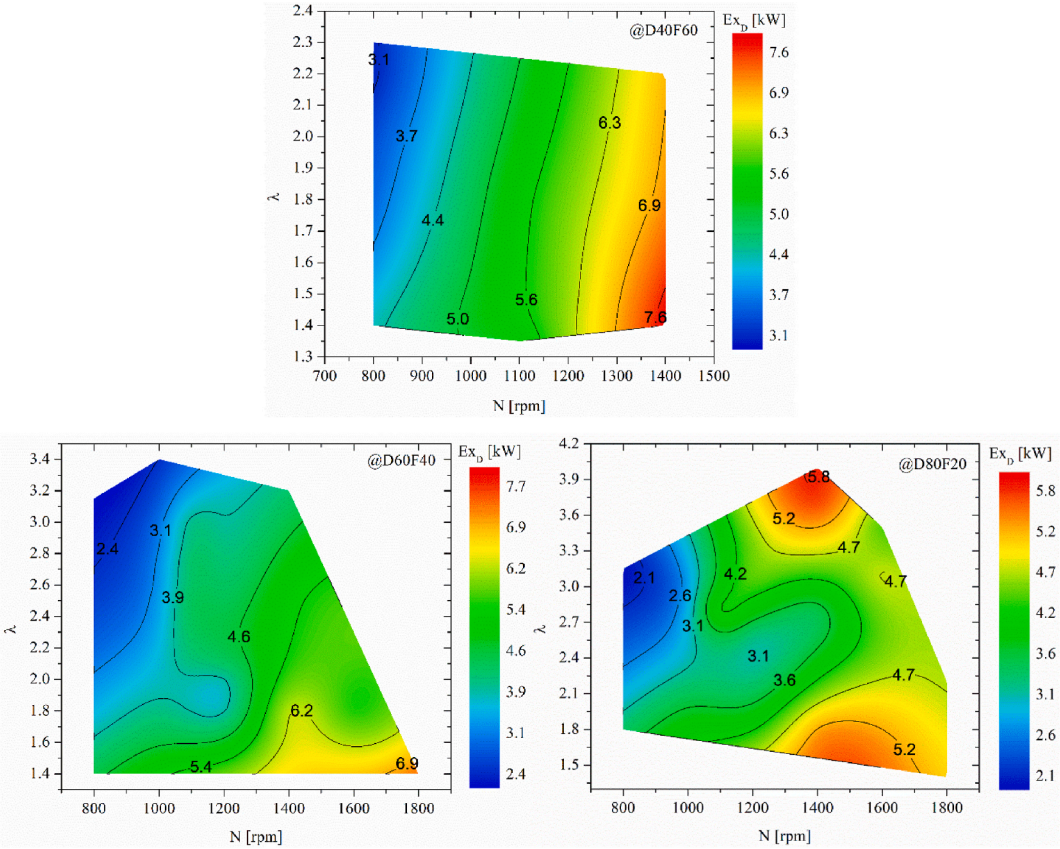

Fig. 5. Exergy destruction rate in relation to lambda and rotational speed.

3. Results and discussions

Fig. 3 presents the average results of the exergy balance of all operating conditions evaluated in this work. The exergy fraction of each test fuel was calculated by dividing the amount of particular exergy into the entry fuel exergy [56]. The total losses represent the heat, cooling, and exhaust gas losses of the engine. It is observed that the destruction exergy has the highest percentage of the balance sheet; this indicates that more than 70% of the exergy supplied by the fuel is wasted in the exergy conversion process, being useful between 8 and 15% of the exergy. On the other hand, when comparing fuel blends, it is observed that as the percentage of fusel in the blend increases, the exergy destroyed decreases. This generates an increase in the oxygen content in the mixture, improving the temperature of the combustion chamber, which causes an increase in cylinder pressure, which finally translates into higher useful power output. Moreover, a higher percentage of fusel in the blends provides an increase in the density and viscosity of the fuel, which reduces the effects of friction and the process of converting chemical energy into heat energy of flue gas and decreases the irreversibilities of the system.

Fig. 4 presents the variation of power output with respect to rotational speed and lambda for the fuels tested. It is observed that with increasing engine rotational speed, the power increases for all the blends tested. In addition, it is observed that the lambda presents different points of maximum power, especially when operating at high rotational speeds. However, when operating with D80F20 a more dispersed distribution of the power output is observed, obtaining a maximum value of 0.62 kW at 1400 rpm and lambda of 3.9. On the other hand, the increase of diethylether in the blend decreases the maximum power output at the operating conditions. This is since HCCI engines present considerable amounts of unburned fuel in the exhaust gases, the latter because of the low combustion temperatures that prevent the oxidation reactions from being completed and the presence of fuel in the cooler areas of the combustion chamber. In addition, the decrease of fusel oil in the mixture decreases the percentage of oxygen in the fuel, obtaining a lower LHV and in turn, decreasing combustion efficiency.

Fig. 5 presents the variation of the exergy destruction rate with respect to rotational speed and lambda for the fuels tested. The figure shows that the rate of exergy destroyed is mainly concentrated at the lower lambda values for D40F60 and D60F40 fuels. However, when operating with D80F20, a higher exergy destruction rate is observed between lambda 3.4 and 3.9. It should be noted that the high values of exergy destruction rate are due to load regulation, which in HCCI engines depends on the amount of fuel injected into the cylinder. The points with higher exergy destruction rate show high load levels, therefore, there is a higher fuel consumption and in perspective, the disproportionate fuel consumption presents higher irreversibilities in the combustion process. On the other

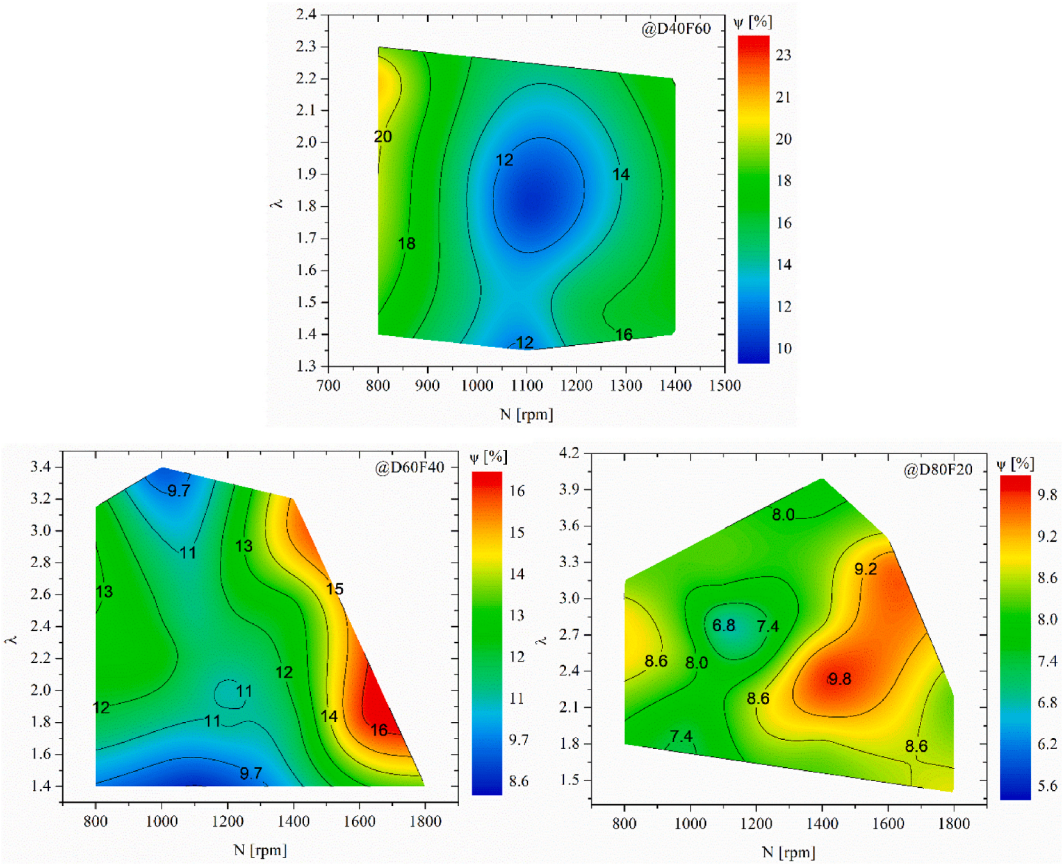

Fig. 6. Exergy efficiency in relation to lambda and rotational speed.

hand, the change of fuel blend alters the ignition point, since HCCI engines control the ignition timing and combustion rate from chemical ratios, turbulence and air-fuel mixture. Therefore, significant differences in fuel behavior are observed even under the same operating conditions.

Fig. 6 shows the variation of the exergy efficiency with respect to rotational speed and lambda for the fuels tested. It is observed that depending on the fuel tested, different points of maximum efficiency are presented. The maximum value of exergy efficiency is 23.85%, with the D80F20 fuel obtaining the lowest values and the D40F60 fuel obtaining the highest values. Additionally, it is shown that the zone with the highest exergy efficiency for all fuels is between lambdas 2.1 to 2.6. As mentioned above, the effect of the fuel mixture alters the ignition point due to the physicochemical properties of the fuel, affecting the combustion efficiency. In addition, oxygenated biofuels such as fusel and diethylether could theoretically improve ignition control. However, the low oxygen content in the blends and the decreased fusel content affect the ignition point. On the other hand, it is observed that there is a more proportional distribution of average and maximum efficiency zones operating with D80F20 compared to D40F60 and D60F40 fuels. This leads to the conclusion that the fuel with a higher percentage of diethylether operates more uniformly under the operating conditions evaluated.

4. Conclusion

In this study, the performance of a HCCI engine powered with D40F60, D60F40, and D80F20 at different engine speeds and lambda values was assessed by exergy indicators. The main conclusions based on the derived results and experimental data could be summarized as follows:

- It is concluded that the lambda variation allows observing the best performance zones when operating with fuel mixtures. However, for future works it is expected to operate the HCCI engine with variable load and measure the pressure in the chamber. In order to identify the areas where the best combustion occurs to obtain a homogeneous mixture and increase engine performance.
- From the comparison of the exergy indicators, it is concluded that the highest engine 2nd law efficiency is obtained when operating with D40F60 at a lambda between 2.1 and 2.2. Likewise, it was determined that the increase of diethyl ether in the blend decreases the performance, since, when operating with D60F40 and D80F20 the variation in the results is significant.
- The fuels tested allowed us to observe that the performance of the HCCI engine shows favorable results, even with fuels that are little used in its operation, obtaining high efficiency values when operating with high fusel content in the mixture, mainly because of the oxygen content, resulting in an increase in the combustion efficiency in low/high load areas. In addition, according to the

results, the effect on the environment was achieved to be neglectable. However, greater stability of performance was observed when operating with D80F20, which indicates that a more uniform combustion temperature was obtained with different lambda values, thus leaving open the discussion on the feasibility of the application of these fuels.

Credit author statement

Juan Zapata-Mina: Methodology, Software, Writing - Original Draft, Writing - Review & Editing, **Seyed Mohammad Safieddin Ardebili:** Methodology, Software, Writing - Original Draft, **Alvaro Restrepo:** Supervision, Writing - Review & Editing, **Hamit Solmaz:** Methodology, Software, Writing - Original Draft, Experimental Implementation **Alper Calam:** Methodology, Investigation, Data collection, Experimental Implementation Writing - Review & Editing, **Özer Can:** Supervision, Conceptualization, Methodology, Writing - Original Draft.

Declaration of competing interest

The authors declare that they have no known competing financial interests or personal relationships that could have appeared to influence the work reported in this paper.

Acknowledgement

This study was funded by Gazi University Scientific Investigation Projects (BAP) with the project code of 07/2019-14. We thank the Gazi University Projects of Scientific Investigation (BAP) and the LPEA of Technological University of Pereira.

References

[1] T.T. Calam, Electrochemical oxidative determination and electrochemical behavior of 4-Nitrophenol based on an Au electrode modified with electro-polymerized 3, 5-diamino-1, 2, 4-triazole film, Electroanalysis 32 (1) (2020) 149–158.
[2] T. Tabanlıgil Calam, Electrochemical behavior and voltammetric determination of 2-Nitrophenol on glassy carbon electrode surface modified with 1-Amino-2-Naphthol-4-sulphonic Acid, Eng. Perspect. 1 (1) (2021) 1–5, https://doi.org/10.29228/sciperspective.48525.
[3] T.T. Calam, Investigation of the electrochemical behavior of phenol using 1H-1, 2, 4-triazole-3-thiol modified gold electrode and its voltammetric determination, J. Facul. Eng.Architect.Gazi .Univ. 35 (2) (2020) 835–844.
[4] T. Tabanlıgil Calam, E.B. Yılmaz, Electrochemical determination of 8-hydroxyquinoline in a cosmetic product on a glassy carbon electrode modified with 1-amino-2-naphthol-4-sulphonic acid, Instrum. Sci. Technol. 49 (1) (2021) 1–20.
[5] T. Tabanlıgil Calam, Analytical application of the poly (1H-1, 2, 4-triazole-3-thiol) modified gold electrode for high-sensitive voltammetric determination of catechol in tap and lake water samples, Int. J. Environ. Anal. Chem. 99 (13) (2019) 1298–1312.
[6] S. Polat, A. Uyumaz, H. Solmaz, E. Yilmaz, T. Topgül, H.S. Yücesu, A numerical study on the effects of EGR and spark timing to combustion characteristics and NO x emission of a GDI engine, Int. J. Green Energy 13 (1) (2016) 63–70.
[7] A. Uyumaz, B. Aydoğan, A. Calam, F. Aksoy, E. Yılmaz, The effects of diisopropyl ether on combustion, performance, emissions and operating range in a HCCI engine, Fuel 265 (2020) 116919.
[8] A. Böğrek, C. Haşimoğlu, A. Calam, B. Aydoğan, Effects of n-heptane/toluene/ethanol ternary fuel blends on combustion, operating range and emissions in premixed low temperature combustion, Fuel 295 (2021) 120628.
[9] B. Aydoğan, An experimental examination of the effects of n-hexane and n-heptane fuel blends on combustion, performance and emissions characteristics in a HCCI engine, Energy 192 (2020) 116600.
[10] S.M.S. Ardebili, A. Calam, E. Yılmaz, H. Solmaz, A comparative analysis of the engine performance and exhaust emissions characteristics of a diesel engine fueled with Mono ethylene glycol supported emulsion, Fuel 288 (2021) 119723.
[11] B. Aydoğan, Combustion, performance and emissions of ethanol/n heptane blends in HCCI engine, Eng. Perspect. 1 (1) (2021) 6–10.
[12] S. Köse, M. Babagiray, T. Kocakulak, Response surface method based optimization of the viscosity of waste cooking oil biodiesel, Eng. Perspect. 1 (1) (2021) 30–37.
[13] E. Yılmaz, A comparative study on the usage of RON68 and Naphtha in an HCCI engine, Int. J. Automot. Sci. Technol. 4 (2) (2020) 90–97.
[14] S.C. Kong, C.D. Marriott, R.D. Reitz, M. Christensen, Modeling and experiments of HCCI engine combustion using detailed chemical kinetics with multidimensional CFD, SAE Trans. (2001) 1007–1018.
[15] S.C. Kong, A study of natural gas/DME combustion in HCCI engines using CFD with detailed chemical kinetics, Fuel 86 (10–11) (2007) 1483–1489.
[16] P.W. Bessonette, C.H. Schleyer, K.P. Duffy, W.L. Hardy, M.P. Liechty, Effects of fuel property changes on heavy-duty HCCI combustion, SAE Trans. (2007) 242–254.
[17] Y. Cui, H. Liu, C. Geng, Q. Tang, L. Feng, Y. Wang, M. Yao, Optical diagnostics on the effects of fuel properties and coolant temperatures on combustion characteristic and flame development progress from HCCI to CDC via PPC, Fuel 269 (2020) 117441.
[18] J.A. Eng, Characterization of Pressure Waves in HCCI Combustion (No. 2002-01-2859, SAE Technical Paper, 2002.
[19] B. Bahri, A.A. Aziz, M. Shahbakhti, M.F.M. Said, Understanding and detecting misfire in an HCCI engine fuelled with ethanol, Appl. Energy 108 (2013) 24–33.
[20] A. Calam, Effects of the fusel oil usage in HCCI engine on combustion, performance and emission, Fuel 262 (2020) 116503.
[21] H. Solmaz, A comparative study on the usage of fusel oil and reference fuels in an HCCI engine at different compression ratios, Fuel 273 (2020) 117775.
[22] P. Das, P.M.V. Subbarao, J.P. Subrahmanyam, Control of combustion process in an HCCI-DI combustion engine using dual injection strategy with EGR, Fuel 159 (2015) 580–589.
[23] C. Li, L. Yin, S. Shamun, M. Tuner, B. Johansson, R. Solsjo, X.S. Bai, Transition from HCCI to PPC: the Sensitivity of Combustion Phasing to the Intake Temperature and the Injection Timing with and without EGR (No. 2016-01-0767), SAE Technical Paper, 2016.
[24] S. Polat, H. Solmaz, E. Yılmaz, A. Calam, A. Uyumaz, H.S. Yücesu, Mapping of an HCCI engine using negative valve overlap strategy, Energy Sources, Part A Recovery, Util. Environ. Eff. 42 (9) (2020) 1140–1154.
[25] S. Polat, H. Solmaz, A. Uyumaz, A. Calam, E. Yılmaz, H. Serdar Yucesu, An experimental research on the effects of Negative valve overlap on performance and operating range in a homogeneous charge compression ignition engine with RON40 and RON60 fuels, J. Eng. Gas Turbines Power 142 (5) (2020).
[26] E. Neshat, R.K. Saray, S. Parsa, Numerical analysis of the effects of reformer gas on supercharged n-heptane HCCI combustion, Fuel 200 (2017) 488–498.
[27] Y. Putrasari, N. Jamsran, O. Lim, An investigation on the DME HCCI autoignition under EGR and boosted operation, Fuel 200 (2017) 447–457.
[28] A. Calam, H. Solmaz, E. Yılmaz, Y. İçingür, Investigation of effect of compression ratio on combustion and exhaust emissions in A HCCI engine, Energy 168 (2019) 1208–1216.
[29] A. Calam, Study on the combustion characteristics of acetone/n-heptane blend and RON50 reference fuels in an HCCI engine at different compression ratios, Fuel 271 (2020) 117646.

[30] M. Parthasarathy, S. Ramkumar, J.I.J. Lalvani, P.V. Elumalai, B. Dhinesh, R. Krishnamoorthy, S. Thiyagarajan, Performance analysis of HCCI engine powered by tamanu methyl ester with various inlet air temperature and exhaust gas recirculation ratios, Fuel 282 (2020) 118833.
[31] B. Aydoğan, Experimental investigation of tetrahydrofuran combustion in homogeneous charge compression ignition (HCCI) engine: effects of excess air coefficient, engine speed and inlet air temperature, J. Energy Inst. 93 (3) (2020) 1163–1176.
[32] S.V. Khandal, N.R. Banapurmath, V.N. Gaitonde, Performance studies on homogeneous charge compression ignition (HCCI) engine powered with alternative fuels, Renew. Energy 132 (2019) 683–693.
[33] T.W. Ryan, T.J. Callahan, D. Mehta, HCCI in a Variable Compression Ratio Engine-Effects of Engine Variables (No. 2004-01-1971), SAE Technical Paper, 2004.
[34] C. Cinar, A. Uyumaz, H. Solmaz, F. Sahin, S. Polat, E. Yilmaz, Effects of intake air temperature on combustion, performance and emission characteristics of a HCCI engine fueled with the blends of 20% n-heptane and 80% isooctane fuels, Fuel Process. Technol. 130 (2015) 275–281.
[35] R.K. Maurya, A.K. Agarwal, Experimental investigations of performance, combustion and emission characteristics of ethanol and methanol fueled HCCI engine, Fuel Process. Technol. 126 (2014) 30–48.
[36] Z. Wang, H. Liu, X. Ma, J. Wang, S. Shuai, R.D. Reitz, Homogeneous charge compression ignition (HCCI) combustion of polyoxymethylene dimethyl ethers (PODE), Fuel 183 (2016) 206–213.
[37] A. Uyumaz, An experimental investigation into combustion and performance characteristics of an HCCI gasoline engine fueled with n-heptane, isopropanol and n-butanol fuel blends at different inlet air temperatures, Energy Convers. Manag. 98 (2015) 199–207.
[38] S. Jafarmadar, P. Nemati, Exergy analysis of diesel/biodiesel combustion in a homogenous charge compression ignition (HCCI) engine using three-dimensional model, Renew. Energy 99 (2016) 514–523.
[39] A.K. Amjad, R.K. Saray, S.M.S. Mahmoudi, A. Rahimi, Availability analysis of n-heptane and natural gas blends combustion in HCCI engines, Energy 36 (12) (2011) 6900–6909.
[40] H. Taghavifar, A. Nemati, J.H. Walther, Combustion and exergy analysis of multi-component diesel-DME-methanol blends in HCCI engine, Energy 187 (2019) 115951.
[41] J. Zhang, Z. Huang, D. Han, Exergy losses in auto-ignition processes of DME and alcohol blends, Fuel 229 (2018) 116–125.
[42] S. Jafarmadar, P. Nemati, Multidimensional modeling of the effect of exhaust gas recirculation on exergy terms in a homogenous charge compression ignition engine fueled by diesel/biodiesel, J. Clean. Prod. 161 (2017) 720–734.
[43] R. Hegner, B. Atakan, A polygeneration process concept for HCCI-engines–Modeling product gas purification and exergy losses, Int. J. Hydrogen Energy 42 (2) (2017) 1287–1297.
[44] E. Neshat, R.K. Saray, V. Hosseini, Effect of reformer gas blending on homogeneous charge compression ignition combustion of primary reference fuels using multi zone model and semi detailed chemical-kinetic mechanism, Appl. Energy 179 (2016) 463–478.
[45] A. Eyal, L. Tartakovsky, Second-law analysis of the reforming-controlled compression ignition, Appl. Energy 263 (2020) 114622.
[46] Y. Icingur, A. Calam, The effects of the blends of fusel oil and gasoline on performance and emissions in a spark ignition engine, J. Facul. Eng.Architect.Gazi . Univ. 27 (1) (2012) 143–149.
[47] S.M.S. Ardebili, H. Solmaz, D. İpci, A. Calam, M. Mostafaei, A review on higher alcohol of fusel oil as a renewable fuel for internal combustion engines: applications, challenges, and global potential, Fuel 279 (2020) 118516.
[48] A. Ibrahim, Investigating the effect of using diethyl ether as a fuel additive on diesel engine performance and combustion, Appl. Therm. Eng. 107 (2016) 853–862.
[49] J. Zapata-Mina, A. Restrepo, C. Romero, H. Quintero, Exergy analysis of a diesel engine converted to spark ignition operating with diesel, ethanol, and gasoline/ethanol blends, Sustain. Energy Technol. Assessments 42 (2020) 100803.
[50] J. Szargut, D.R. Morris, F.R. Steward, Exergy Analysis of Thermal, Chemical, and Metallurgical Processes. New York, USA, 1987.
[51] T. Kotas, The Exergy Method of Thermal Plant Analysis. London, UK, 2013.
[52] H. Caliskan, K. Mori, Thermodynamic, environmental and economic effects of diesel and biodiesel fuels on exhaust emissions and nano-particles of a diesel engine, Transport. Res. Transport Environ. 56 (2017) 203–221.
[53] B. Doğan, D. Erol, H. Yaman, E. Kodanli, The effect of ethanol-gasoline blends on performance and exhaust emissions of a spark ignition engine through exergy analysis, Appl. Therm. Eng. 120 (2017) 433–443.
[54] G. Khoobbakht, A. Akram, M. Karimi, G. Najafi, Exergy and energy analysis of combustion of blended levels of biodiesel, ethanol and diesel fuel in a DI diesel engine, Appl. Therm. Eng. 99 (2016) 720–729.
[55] O. Balli, Y. Sohret, H.T. Karakoc, The effects of hydrogen fuel usage on the exergetic performance of a turbojet engine, Int. J. Hydrogen Energy 43 (23) (2018) 10848–10858.
[56] M. Hoseinpour, H. Sadrnia, M. Tabasizadeh, B. Ghobadian, Energy and exergy analyses of a diesel engine fueled with diesel, biodiesel-diesel blend and gasoline fumigation, Energy 141 (2017) 2408–2420.